
Nonlinear FEM

Total Lagrange method

by:

Lucas Silveira
October 14, 2021

1 Finite strain theory

Figure 1 illustrates a body \mathcal{B} before (a) and after (b) it undergoes a macroscopic displacement \mathbf{u} composed of a rigid body translation, rotation and deformation. As is the convention in continuum mechanics, the vector \mathbf{X} is used to define a particle position in the undeformed configuration and the vector \mathbf{x} its position after deformation.

In the material or Lagrangian description, the body kinematics is referred to and analysed in reference configuration κ_R , which is the undeformed configuration in the Total Lagrange Formulation or the previous converged time step in the Updated Lagrange Formulation.

$$\mathbf{x} = \mathcal{X}(\mathbf{X}, t) \quad (1)$$

$$\mathbf{u} = \mathbf{u}(\mathbf{X}, t) = \mathbf{x}(\mathbf{X}, t) - \mathbf{X} \quad (2)$$

1.1 Deformation gradient tensor

A key concept in finite deformation analysis is the displacement gradient tensor \mathbf{F} , given by the derivative of the spatial coordinates with respect its material coordinates. The displacement gradient tensor characterizes the local deformation by relating an infinitesimal material line $d\mathbf{X}$ before deformation to the line $d\mathbf{x}$ after deformation

$$\mathbf{F} = \frac{\partial \mathbf{x}}{\partial \mathbf{X}} = \frac{\partial \mathbf{u}}{\partial \mathbf{X}} + \mathbf{I} \quad (3)$$

$$d\mathbf{x} = \mathbf{F} d\mathbf{X} \quad (4)$$

$$d\mathbf{X} = \mathbf{F}^{-1} d\mathbf{x} \quad (5)$$

1.1.1 Volume change

Figure 2 illustrates a parallelepiped volume element before and after a finite displacement. In the initial configuration, the edges of the parallelepiped volume are formed by three line elements $d\mathbf{X}_1$, $d\mathbf{X}_2$ and $d\mathbf{X}_3$ and its undeformed volume is given by the triple product in Equation (6).

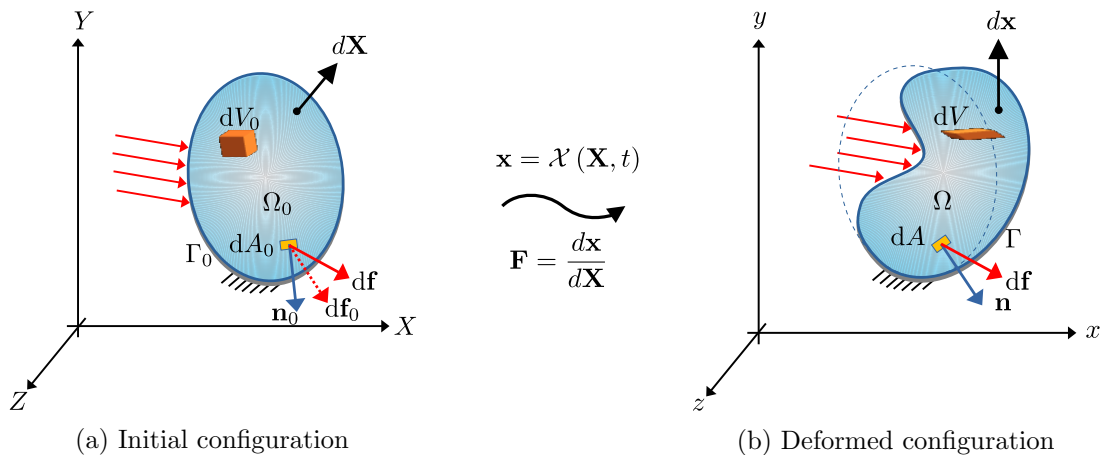


Figure 1

$$dV_0 = (d\mathbf{X}_1 \times d\mathbf{X}_2) \cdot d\mathbf{X}_3 = dX_1 dX_2 dX_3 \quad (6)$$

Similarly, the edges of the deformed volume are formed by the deformed line elements \mathbf{x}_1 , \mathbf{x}_2 and \mathbf{x}_3 and the deformed volume is given by their triple product, Equation (7). Inserting Equation (4) into Equation (7), it is shown that the determinant of the deformation gradient tensor $\det(\mathbf{F})$ represents the ratio between the reference volume and the current volume.

$$\begin{aligned} dV &= (d\mathbf{x}_1 \times d\mathbf{x}_2) \cdot d\mathbf{x}_3 = [(\mathbf{F}d\mathbf{X}_1) \times (\mathbf{F}d\mathbf{X}_2)] \cdot (\mathbf{F}d\mathbf{X}_3) \\ &= F_{i1}F_{j2}F_{k3}\epsilon_{ijk}dX_1dX_2dX_3 \\ &= \det(\mathbf{F})dV_0 \end{aligned} \quad (7)$$

1.1.2 Area change

Also illustrated on Figure 2 is the parallelogram area element before and after a finite displacement. In the initial configuration, the edges of the parallelogram area are formed by two line elements $d\mathbf{X}_1$ and $d\mathbf{X}_2$. The undeformed surface vector $d\mathbf{A}_0 = dA_0\mathbf{n}_0$, where \mathbf{n}_0 is the unit vector normal to the undeformed area element, is given by the vector product between the undeformed line elements. Similarly the deformed surface vector $d\mathbf{A}$ is given by the vector product between the deformed line elements $d\mathbf{x}_1$ and $d\mathbf{x}_2$.

$$d\mathbf{A}_0 = d\mathbf{X}_1 \times d\mathbf{X}_2 \quad (8)$$

$$d\mathbf{A} = d\mathbf{x}_1 \times d\mathbf{x}_2 \quad (9)$$

The undeformed and deformed volume elements can be expressed in terms of the scalar product between the surface vectors and $d\mathbf{X}_3$ or $d\mathbf{x}_3$ respectively.

$$dV_0 = d\mathbf{A}_0 \cdot d\mathbf{X}_3 \quad (10)$$

$$dV = d\mathbf{A} \cdot d\mathbf{x}_3 \quad (11)$$

Inserting Equations (10) and (11) into Equation (7) and solving for $d\mathbf{A}$, it can be shown the relation between $d\mathbf{A}$ and $d\mathbf{A}_0$ is given by Equation (13).

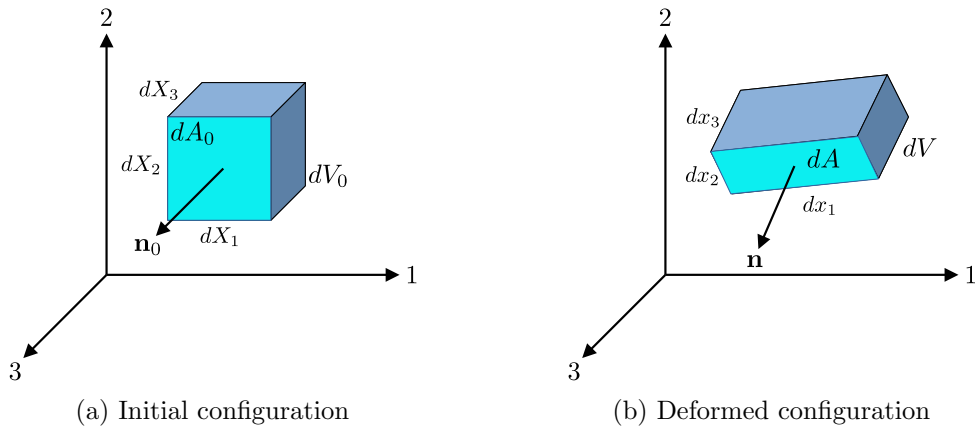


Figure 2

$$d\mathbf{A} \cdot (\mathbf{F}d\mathbf{X}_3) = \det(\mathbf{F}) d\mathbf{A}_0 \cdot d\mathbf{X}_3 \quad (12)$$

$$d\mathbf{A} = \det(\mathbf{F}) \mathbf{F}^{-T} d\mathbf{A}_0 \quad (13)$$

1.1.3 Polar decomposition

As any invertible matrix, the deformation gradient tensor \mathbf{F} may be decomposed into the product of an unitary matrix \mathbf{R} and a right or left Hermitian matrix \mathbf{U} or \mathbf{V} . The unitary matrix \mathbf{R} represent the rigid body rotation component of the deformation gradient tensor and the left and right Hermitian matrices \mathbf{U} and \mathbf{V} represent its pure deformation component, the left and right meaning the transformation order. Figure 3 illustrates the polar decomposition of the deformation gradient tensor applied to an infinitesimal solid.

$$\mathbf{F} = \mathbf{R}\mathbf{U} = \mathbf{V}\mathbf{R} \quad (14)$$

1.2 Green-Lagrange strain

The Green-Lagrange strain tensor is defined in terms of the displacement derivative tensor or the deformation gradient tensor trough Equation (15).

$$\mathbf{E} = \frac{1}{2} (\mathbf{F}^T \mathbf{F} - \mathbf{I}) = \frac{1}{2} \left[\left(\frac{\partial \mathbf{u}}{\partial \mathbf{X}} \right) + \left(\frac{\partial \mathbf{u}}{\partial \mathbf{X}} \right)^T + \left(\frac{\partial \mathbf{u}}{\partial \mathbf{X}} \right)^T \left(\frac{\partial \mathbf{u}}{\partial \mathbf{X}} \right) \right] \quad (15)$$

From Equation (15), one can observe the Green-Lagrange strain tensor is formed by the Cauchy strain plus quadratic terms, which are ignored in small displacement theory. An important property of the Green-Lagrange strain tensor is that, unlike the Cauchy strain tensor, it is rotation-invariant as the product $\mathbf{F}^T \mathbf{F}$ eliminates the the rigid body rotation component \mathbf{R} component deformation gradient tensor.

$$\mathbf{F}^T \mathbf{F} = \mathbf{U}^T \mathbf{R}^T \mathbf{R} \mathbf{U} = \mathbf{U}^T \mathbf{U} \quad (16)$$

The physical meaning of the Green-Lagrange strain tensor is not as straightforward as for the Cauchy strain. While the Cauchy is related to the change of length of a line element $d\mathbf{x}$, the Green-Lagrange strain is related to the change of its square.

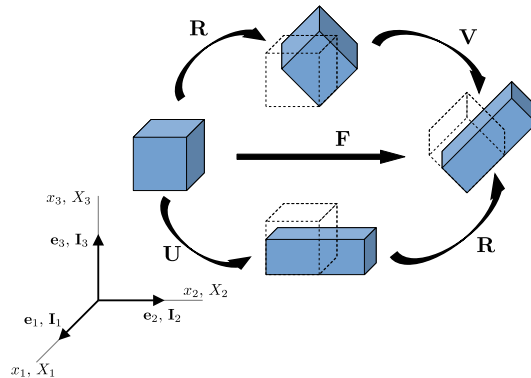


Figure 3: Representation of the polar decomposition of the deformation gradient.

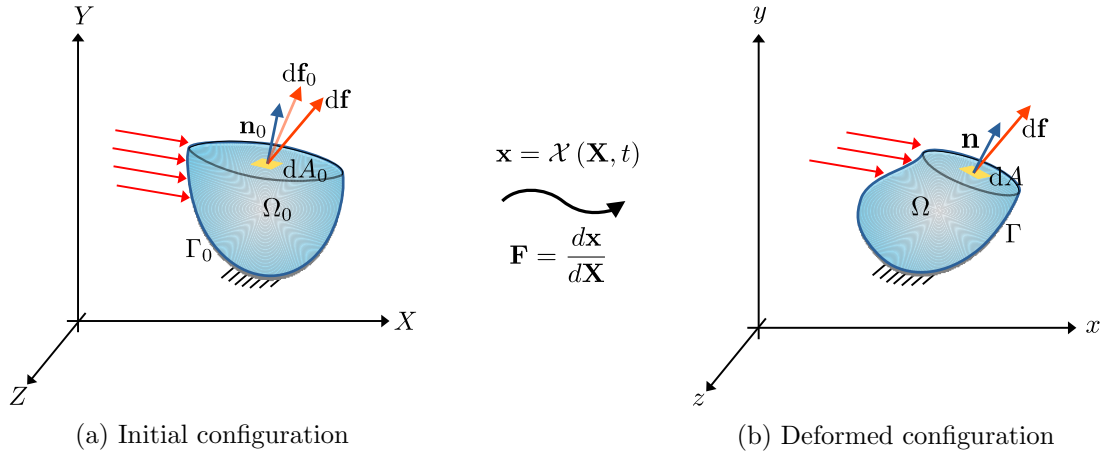


Figure 4: First and Second Piola Kirchhoff stress tensors

$$\frac{1}{2} (d\mathbf{x}^T d\mathbf{x} - d\mathbf{X}^T d\mathbf{X}) = d\mathbf{X}^T \mathbf{E} d\mathbf{X} \quad (17)$$

1.3 Stress measures

1.3.1 First Piola Kirchhoff stress tensor

The Cauchy stress tensor $\boldsymbol{\sigma}$ or true stress is the most natural and physical measure of the stress distribution in the deformed configuration. However, the geometry of the deformed is one of the problem unknowns. In the total Lagrange approach, the equilibrium equations are written in terms of the known reference configuration and new stress measurements are needed. They result naturally from the projection of quantities from the deformed to the reference configuration through the deformation gradient tensor \mathbf{F} . They should be seen as mathematical quantities which facilitate the analysis but which lack the same physical meaning of the Cauchy stress tensor.

Figure 4 illustrates a section of a continuous body \mathcal{B} subjected to a displacement mapping \mathcal{X} . The internal force $d\mathbf{f}$ acting on an area element dA with normal \mathbf{n} is given by Equation 18 where $\boldsymbol{\sigma}$ is the Cauchy stress tensor. The first Piola Kirchhoff stress tensor \mathbf{P} is defined in such a way that its product with the reference normal \mathbf{n}_0 and area dA_0 result in the same force vector $d\mathbf{f}$.

$$d\mathbf{f} = \boldsymbol{\sigma} \mathbf{n} dA = \mathbf{P} \mathbf{n}_0 dA_0 \quad (18)$$

Inserting Equation (13) into Equation (18) and rearranging, the first Piola Kirchhoff is given by Equation (19)

$$\mathbf{P} = \det(\mathbf{F}) \boldsymbol{\sigma} \mathbf{F}^{-T} \quad (19)$$

The First Piola Kirchhoff is related to the engineering stress (force over initial area) and the surface normal in the reference configuration. Despite this relation, the First Piola Kirchhoff is rarely used since, unlike the Cauchy stress, it is not symmetric.

1.3.2 Second Piola Kirchhoff stress tensor

The Second Piola Kirchhoff introduces the definition of transformed current force or pulled-back force $d\mathbf{f}_0$. As the reference line segment $d\mathbf{X}$ is related to the current line segment $d\mathbf{x}$ through Equation (5), the pulled-back force $d\mathbf{f}_0$ is related to the current force vector through Equation (20).

$$d\mathbf{f}_0 = \mathbf{F}^{-1}d\mathbf{f} \quad (20)$$

The transformed current force $d\mathbf{f}_0$ is a mathematical convenience and has no strict physical meaning. As the First Piola Kirchhoff stress tensor \mathbf{P} is related to the current force $d\mathbf{f}$ through Equation (18), the Second Piola Kirchhoff stress tensor \mathbf{S} is related to the pulled-back force vector through Equation (21).

$$d\mathbf{f}_0 = \mathbf{S}\mathbf{n}_0dA_0 \quad (21)$$

Inserting Equations (18), (19) and (20) into Equation (21) and solving for \mathbf{S} , one obtains the Second Piola Kirchhoff is related to the Cauchy stress tensor by:

$$\mathbf{S} = \mathbf{F}^{-1}\mathbf{P} = \det(\mathbf{F})\mathbf{F}^{-1}\boldsymbol{\sigma}\mathbf{F}^{-T} \quad (22)$$

1.4 Equations of motion

Figures 1a and 1b illustrates an continuum body \mathcal{B} in the reference and current configurations respectively. The equation of motion of body \mathcal{B} is given by

$$\int_{\Gamma} \boldsymbol{\sigma}\mathbf{n}dA + \int_{\Omega} \mathbf{b}dV = \int_{\Omega} \rho\ddot{\mathbf{u}}dV \quad (23)$$

where the first term describes the surface forces acting on its boundaries, the second term includes the body forces acting throughout its volume and the right-hand side term describe the body inertia. As described in section 1.3.1, even though the equations of motion have physical meaning on the current configuration where the body displacement is unknown, large strain and stress measures can be used to rewrite the equation of motion in the reference configuration. The equation of motion of body \mathcal{B} in the reference configuration is given by

$$\int_{\Gamma_0} \mathbf{P}\mathbf{n}_0dA_0 + \int_{\Omega_0} \mathbf{b}_0dV_0 = \int_{\Omega_0} \rho\ddot{\mathbf{u}}dV_0 \quad (24)$$

where \mathbf{P} is the First Piola Kirchhoff stress tensor and the body force density \mathbf{b}_0 in the reference configuration is given by the relation

$$\mathbf{b}_0 = \mathbf{b}\det(\mathbf{F}) \quad (25)$$

Applying the divergence theorem on the first term of Equation (24) and premultiplying it by a virtual displacement $\delta\mathbf{u}$, the equation of motion can be rewritten as

$$\int_{\Omega_0} \delta\mathbf{u} \cdot \operatorname{div}_X(\mathbf{P})dV_0 + \int_{\Omega_0} \delta\mathbf{u} \cdot \mathbf{b}_0dV_0 = \int_{\Omega_0} \delta\mathbf{u} \cdot \rho\ddot{\mathbf{u}}dV_0 \quad (26)$$

The first term on Equation (26) can be integrated by parts to yield

$$\begin{aligned}
\int_{\Omega_0} \delta u_i \frac{\partial P_{ij}}{\partial X_j} dV_0 &= \int_{\Gamma_0} \delta u_i P_{ij} n_{0,j} dA_0 - \int_{\Omega_0} \frac{\partial \delta u_i}{\partial X_j} P_{ij} dV_0 \\
&= \int_{\Gamma_0} \delta \mathbf{u} \cdot (\mathbf{P} \cdot \mathbf{n}_0) dA_0 - \int_{\Omega_0} \frac{\partial \delta \mathbf{u}}{\partial \mathbf{X}} : \mathbf{P} dV_0 \\
&= \int_{\Gamma_0} \delta \mathbf{u} \cdot \mathbf{t}_0 dA_0 - \int_{\Omega_0} \delta \mathbf{F} : \mathbf{P} dV_0
\end{aligned} \tag{27}$$

where the relation in Equation (28) was used.

$$\delta \mathbf{F} = \delta \left[\mathbf{I} + \frac{\partial \mathbf{u}}{\partial \mathbf{X}} \right] = \frac{\partial \delta \mathbf{u}}{\partial \mathbf{X}} \tag{28}$$

Finally, the deformation gradient tensor and the First Piola-Kirchhoff strain tensor in the second term of Equation (28) can be replaced by the Green Lagrange strain tensor and the Second Piola-Kirchhoff stress tensor power conjugate through the \mathbf{S} symmetry.

$$\begin{aligned}
\delta \mathbf{F} : \mathbf{P} &= \delta \mathbf{F} : (\mathbf{F} \mathbf{S}) = (\mathbf{F}^T \delta \mathbf{F}) : \mathbf{S} \\
&= (\mathbf{F}^T \delta \mathbf{F})_{sym} : \mathbf{S} \\
&= \frac{1}{2} [\mathbf{F}^T \delta \mathbf{F} + \delta \mathbf{F}^T \mathbf{F}] : \mathbf{S} \\
&= \delta \mathbf{E} : \mathbf{S}
\end{aligned} \tag{29}$$

Finally, inserting Equations (27), (28) and (29) into Equation (26), one obtains the weak form of the equilibrium equation or the principle of the virtual work in the reference configuration.

$$\underbrace{\int_{\Omega_0} \rho \delta \mathbf{u} \cdot \ddot{\mathbf{u}} dV_0}_{\delta W_{kin}} + \underbrace{\int_{\Omega_0} \delta \mathbf{E} : \mathbf{S} dV_0}_{\delta W_{int}} = \underbrace{\int_{\Gamma_0} \delta \mathbf{u} \cdot \mathbf{t}_0 dA_0 + \int_{\Omega_0} \delta \mathbf{u} \cdot \mathbf{b}_0 dV_0}_{\delta W_{ext}} \tag{30}$$

The first term of Equation (30) represents the variation of the bodies kinetic energy as result of the virtual displacement; alternatively it can be interpreted as the virtual work performed by kinetic forces. The second term represents the variation of potential elastic energy with the virtual displacement or the virtual work of internal elastic forces. The right-hand side term represent the virtual work performed surface and body forces respectively.

1.5 Constitutive equation

The Generalized Hook's law for the linear elastic solids without prestress is given by the relation

$$\mathbf{S} = \mathbf{C} : \mathbf{E} \tag{31}$$

where the stiffness coefficient $\mathbf{C} = C_{ijkl}$ is a fourth order tensor. The symmetry of the Second Piola Kirchhoff stress tensor implies the stiffness tensor is symmetric around its first and second indices

$C_{ijkl} = C_{jikl}$. Similarly, due to the Green Lagrange strain tensor symmetry, the stiffness tensor is also symmetric about its third and fourth indices $C_{ijkl} = C_{ijlk}$. Additionally, since the Green Lagrange strain the Second Piola Kirchhoff stress are work conjugates, the constitutive equation can be derived from the strain energy density U_0

$$\delta U_0 = \mathbf{S} : \delta \mathbf{E} \quad (32)$$

$$S_{ij} = \frac{\partial U_0}{\partial E_{ij}} \implies C_{ijkl} = \frac{\partial^2 U_0}{\partial E_{ij} \partial E_{kl}} \quad (33)$$

where the symmetry around the order of differentiation implies that $C_{ijkl} = C_{klij}$. These three symmetries combined reduce the number of independent elastic constants from 81 to 21. The elastic tensor \mathbf{C} can be simplified further if additional symmetries are assumed. For Isotropic materials, whose material properties are independent of the direction, the constitutive relation is given by

$$S_{ij} = \frac{E}{(1 + \nu)} \left[E_{ij} + \frac{\nu}{(1 - 2\nu)} \delta_{ij} E_{mm} \right] \quad (34)$$

where,

$$C_{ijkl} = \frac{E}{(1 + \nu)} \left[\delta_{ik} \delta_{jl} + \frac{\nu}{(1 - 2\nu)} \delta_{ij} \delta_{mk} \delta_{ml} \right] \quad (35)$$

where E and ν are the material Young's Modulus and Poisson's ration respectively. It is usual to represent the constitutive equation using Voigt notation which represents a symmetric tensor by reducing its order.

$$\mathbf{S}_v = \mathbf{C}_v \mathbf{E}_v \quad (36)$$

$$\begin{bmatrix} S_{11} \\ S_{22} \\ S_{33} \\ S_{23} \\ S_{13} \\ S_{12} \end{bmatrix} = \frac{E}{(1 + \nu)(1 - 2\nu)} \begin{bmatrix} 1 - \nu & \nu & \nu & 0 & 0 & 0 \\ \nu & 1 - \nu & \nu & 0 & 0 & 0 \\ \nu & \nu & 1 - \nu & 0 & 0 & 0 \\ 0 & 0 & 0 & \frac{1-2\nu}{2} & 0 & 0 \\ 0 & 0 & 0 & 0 & \frac{1-2\nu}{2} & 0 \\ 0 & 0 & 0 & 0 & 0 & \frac{1-2\nu}{2} \end{bmatrix} \begin{bmatrix} E_{11} \\ E_{22} \\ E_{33} \\ 2E_{23} \\ 2E_{13} \\ 2E_{12} \end{bmatrix} \quad (37)$$

2 Finite element discretisation

Equation (30) can be solved analytically for very special conditions in regular domains under simple loads, engineering problems are usually very complex to be solved analytically. However, if the problem domain is divided into sufficiently small elements, the field variables distribution within a given element can be reasonably approximated by polynomial functions.

Mesh generation is one of the key tasks in order to obtain accurate results from a finite element model. The mesh elements should be small enough to represent the problem geometry and for the polynomial distribution assumption to correctly approximate field variables distribution. Triangular and tetrahedral elements are often used due to their flexibility in representing complex 2D and 3D geometries respectively. Quadrilateral and hexahedral meshes, on the other hand, often require a lower number of nodes.

Figures 5a and 5b illustrate the geometry of a quadrilateral element with nine nodes in its physical and natural coordinates systems respectively. Coordinate mapping is used so that the shape functions and

integration formulas developed for regular rectangular elements and described below can be used for general quadrilateral elements. The Cartesian coordinates, in the reference configuration, of a point inside the element are then given by Equations (38) and (39)

$$X(\xi, \eta) = \sum h_i(\xi, \eta) X_i \quad (38)$$

$$Y(\xi, \eta) = \sum h_i(\xi, \eta) Y_i \quad (39)$$

where X_i and Y_i are the coordinates of node i in the reference configuration and h_i are linearly independent shape functions which assume a value one at node i and a value zero at the other nodes. For a nine node rectangular element, one valid definition of h_i is given by Equation (40)

$$h_i(\xi, \eta) = c_0 + c_1\xi + c_2\eta + c_3\xi\eta + c_4\xi^2 + c_5\eta^2 + c_6\xi\eta^2 + c_7\eta^2\xi + c_8\eta^2\xi^2 \quad (40)$$

where the constants c_0 to c_8 are found solving for $N_i(\xi_j, \eta_j) = \delta_{ij}$ at the nodes. It is straightforward to show that the nine shape functions are then given by Equations (41) to (49).

$$h_0(\xi, \eta) = \frac{1}{4}\eta\xi(\eta-1)(\xi-1) \quad (41)$$

$$h_1(\xi, \eta) = \frac{1}{4}\eta\xi(\eta-1)(\xi+1) \quad (42)$$

$$h_2(\xi, \eta) = \frac{1}{4}\eta\xi(\eta+1)(\xi+1) \quad (43)$$

$$h_3(\xi, \eta) = \frac{1}{4}\eta\xi(\eta+1)(\xi-1) \quad (44)$$

$$h_4(\xi, \eta) = -\frac{1}{2}\eta(\eta-1)(\xi-1)(\xi+1) \quad (45)$$

$$h_5(\xi, \eta) = -\frac{1}{2}\xi(\eta-1)(\eta+1)(\xi+1) \quad (46)$$

$$h_6(\xi, \eta) = -\frac{1}{2}\eta(\eta+1)(\xi-1)(\xi+1) \quad (47)$$

$$h_7(\xi, \eta) = -\frac{1}{2}\xi(\eta-1)(\eta+1)(\xi-1) \quad (48)$$

$$h_8(\xi, \eta) = \eta^2\xi^2 - \eta^2 - \xi^2 + 1 \quad (49)$$

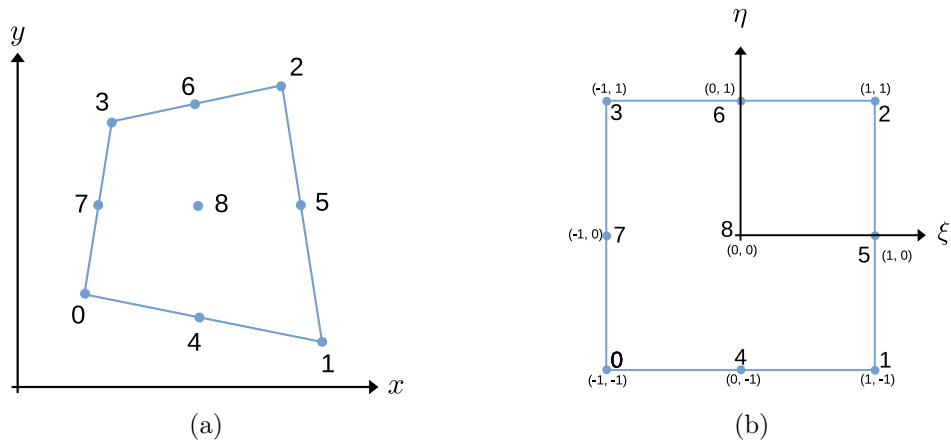


Figure 5: Coordinates mapping of a quadratic quadrilateral element between (a) Physical coordinates system and (b) Natural coordinates system

Similarly, other field variables such as the coordinates in the deformed configuration and the displacement are approximated in terms of their values at the nodes and the shape functions.

$$x(\xi, \eta) = \sum h_i(\xi, \eta) x_i \quad (50)$$

$$y(\xi, \eta) = \sum h_i(\xi, \eta) y_i \quad (51)$$

$$u(\xi, \eta) = \sum h_i(\xi, \eta) u_i \quad (52)$$

$$v(\xi, \eta) = \sum h_i(\xi, \eta) v_i \quad (53)$$

3 Nonlinear finite element formulation

Using equations (52) and (53), the displacement spacial derivative tensor can be expressed in terms of the displacement at the nodal coordinates and the spacial derivatives of the shape functions by equation (54).

$$\frac{\partial \mathbf{u}}{\partial \mathbf{X}} = \begin{bmatrix} \frac{\partial u}{\partial X} & \frac{\partial u}{\partial Y} \\ \frac{\partial v}{\partial X} & \frac{\partial v}{\partial Y} \end{bmatrix} = \begin{bmatrix} \frac{\partial h_i}{\partial X} u_i & \frac{\partial h_i}{\partial Y} u_i \\ \frac{\partial h_i}{\partial X} v_i & \frac{\partial h_i}{\partial Y} v_i \end{bmatrix} = \begin{bmatrix} u_0 & u_1 & u_2 & \cdots \\ v_0 & v_1 & v_2 & \cdots \end{bmatrix} \begin{bmatrix} \frac{\partial h_0}{\partial X} & \frac{\partial h_0}{\partial Y} \\ \frac{\partial h_1}{\partial X} & \frac{\partial h_1}{\partial Y} \\ \frac{\partial h_2}{\partial X} & \frac{\partial h_2}{\partial Y} \\ \vdots & \vdots \end{bmatrix} = \mathbf{U}_e^T \mathbf{GN} \quad (54)$$

The mode shapes are usually defined in terms of the element natural coordinates. The derivatives of the mode shapes with respect with its physical coordinates in the matrix \mathbf{GN} are calculated applying the chain rule

$$\frac{\partial h_i}{\partial X_j} = \frac{\partial h_i}{\partial \xi_k} \frac{\partial \xi_k}{\partial X_j} \quad (55)$$

$$\mathbf{GN} = \mathbf{DN} \mathbf{J}_e^{-1} \quad (56)$$

where the matrix \mathbf{DN} is formed by the derivatives of the mode shapes with respect with its natural coordinates (ξ, η) and the matrix \mathbf{J}_e is given the Jacobian of the element physical coordinates (X, Y) in the reference configuration with respect with its natural coordinates (ξ, η) .

$$\mathbf{DN} = \frac{\partial h_i}{\partial \xi_j} = \begin{bmatrix} \frac{\partial h_0}{\partial \xi} & \frac{\partial h_0}{\partial \eta} \\ \frac{\partial h_1}{\partial \xi} & \frac{\partial h_1}{\partial \eta} \\ \frac{\partial h_2}{\partial \xi} & \frac{\partial h_2}{\partial \eta} \\ \vdots & \vdots \end{bmatrix} \quad (57)$$

$$\mathbf{J}_e = \frac{\partial X_i}{\partial \xi_j} = \begin{bmatrix} \frac{\partial X}{\partial \xi} & \frac{\partial X}{\partial \eta} \\ \frac{\partial Y}{\partial \xi} & \frac{\partial Y}{\partial \eta} \end{bmatrix} \quad (58)$$

Inserting Equation (56) into equation (54), the displacement derivatives are given by Equation (59).

$$\frac{\partial \mathbf{u}}{\partial \mathbf{X}} = \mathbf{U}_e^T \mathbf{D} \mathbf{N} \mathbf{J}_e^{-1} \quad (59)$$

In general, with exception of linear triangular elements, the numerical integration of the weak form of the equilibrium equation is performed numerically through the Gaussian quadrature at specific Gaussian points (ξ_i, η_i) . This means the element Jacobian \mathbf{J}_e need not be inverted analytically, rather evaluated at the correspondent Gaussian points and inverted numerically.

3.1 Elastic forces

The inner product in the internal work equation (30) is often expressed using the Voigt notation where the Green-Lagrange strain and the Second Piola-Kirchhoff stress are written as one dimensional vectors.

$$\delta W_{int} = \int_{\Omega_0} \mathbf{S} : \delta \mathbf{E} dV = \int_{\Omega_0} (\delta \mathbf{E}_v)^T \mathbf{S}_v dV \quad (60)$$

The variation of the Green-Lagrange strain vector $\delta \mathbf{E}_v$ can be written as a function of the variation of the nodal displacements through Equation (61).

$$\delta \mathbf{E}_v = \frac{\partial \mathbf{E}_v}{\partial \mathbf{u}_e} \delta \mathbf{u}_e = \mathbf{B} \delta \mathbf{u}_e \quad (61)$$

$$\mathbf{u}_e = [u_0 \quad v_0 \quad u_1 \quad v_1 \quad u_2 \quad v_2 \quad \dots]^T \quad (62)$$

where the nodal displacement \mathbf{u}_e in vector form is given by equation (62). Different bookkeeping strategies for the derivation of the matrix \mathbf{B} can be found in the literature for various element types, however the process is trivial with the aid of a mathematical symbolic tool or package. Inserting equation (61) into equation (60), the variational work of internal forces is given by equation (63)

$$\delta W_{int} = \delta \mathbf{u}_e^T \int_{\Omega} \mathbf{B}^T \mathbf{S}_v dV = \delta \mathbf{u}_e^T \mathbf{f}_e(\mathbf{u}_e) \quad (63)$$

where the Second Piola-Kirchhoff stress tensor can be calculated from the Green-Lagrange stress tensor through the material constitutive Equation (36). The term inside the integral is the generalised nonlinear internal elastic force vector.

$$\mathbf{f}(\mathbf{u}_e) = \int_{\Omega_0} \mathbf{B}^T \mathbf{S}_v dV_0 \quad (64)$$

The element volume differential in Equation (64) can be expressed in terms of the natural coordinates (ξ, η) the element Jacobian \mathbf{J}_e by the equation

$$dV_0 = h dX dY = h \det(\mathbf{J}_e) d\xi d\eta \quad (65)$$

3.2 Stiffness Matrix

The tangential stiffness matrix \mathbf{K} is derived taking the derivative of the internal elastic forces with respect to the nodal displacements. However, since both terms in the integrand are a function of the

nodal displacement, the stiffness matrix is given by two terms. The first term in equation (66) is referred in the literature as the geometric stiffness while the second is referred as material stiffness.

$$\begin{aligned}\mathbf{K} &= \frac{\partial \mathbf{f}_e}{\partial \mathbf{u}_e} = \int_{\Omega_0} \frac{\partial \mathbf{B}^T}{\partial \mathbf{u}_e} \mathbf{S}_v dV_0 + \int_{\Omega_0} \mathbf{B}^T \frac{\partial \mathbf{S}_v}{\partial \mathbf{u}_e} dV_0 \\ &= \underbrace{\int_{\Omega_0} \frac{\partial \mathbf{B}^T}{\partial \mathbf{u}_e} \mathbf{S}_v dV_0}_{\mathbf{K}_{geo}} + \underbrace{\int_{\Omega_0} \mathbf{B}^T \mathbf{C}_v \mathbf{B} dV_0}_{\mathbf{K}_{mat}}\end{aligned}\quad (66)$$

Again, different bookkeeping strategies for the derivation of the third order tensor $\partial \mathbf{B}^T / \partial \mathbf{u}_e$ can be found in the literature for various element types, however the process is trivial with the aid of a mathematical symbolic tool or package. If the displacements are infinitesimal such that the stress and strain tensors can be approximated by the linear Cauchy stress tensor and engineering strain tensor respectively, the matrix \mathbf{B} becomes independent of the nodal displacement vector \mathbf{u}_e , the geometric stiffness tends to zero and the material stiffness tend to the linear stiffness tensor.

3.3 Mass matrix

The mass matrix is derived from the discretisation of the virtual work of the inertia forces given in equation (30). The displacement field inside the element can be expressed as a function of the nodal displacements and the nodal shape functions by the equation

$$\mathbf{u} = \mathbf{N} \mathbf{u}_e \quad (67)$$

where the matrix \mathbf{N} is given by

$$\mathbf{N} = \begin{bmatrix} h_0(\xi, \eta) & 0 & h_1(\xi, \eta) & 0 & h_2(\xi, \eta) & 0 & \cdots \\ 0 & h_0(\xi, \eta) & 0 & h_1(\xi, \eta) & 0 & h_2(\xi, \eta) & \cdots \end{bmatrix} \quad (68)$$

Inserting Equation (67) into Equation (30) and rearranging, the virtual work of the inertia forces are given by the equation

$$\delta W_{kin} = \int_{\Omega_0} \rho \delta \mathbf{u}^T \ddot{\mathbf{u}} dV = \delta \mathbf{u}_e^T \left(\int_{\Omega_0} \rho \mathbf{N}^T \mathbf{N} dV \right) \ddot{\mathbf{u}}_e = \delta \mathbf{u}_e^T \mathbf{M} \ddot{\mathbf{u}}_e \quad (69)$$

where the mass matrix is given by

$$\mathbf{M} = \int_{\Omega_0} \rho \mathbf{N}^T \mathbf{N} dV \quad (70)$$

In the Total Lagrange Formulation, the undeformed or initial configuration is used as reference configuration. As a consequence, the mass matrix \mathbf{M} is constant even for large displacements, which can be exploited to increase the time integration algorithm speed.

3.4 Surface forces vector

The virtual work performed by external surface forces is given by the first term on the right-hand side of Equation (30). Although quadrilateral and triangular elements can be used in its discretisation, the use of boundary elements significantly simplifies the discretisation process without accuracy loss since the forces are non-zero at the boundaries only. The discretisation of boundary elements follow the same logic described above for quadrilateral elements. Inserting the discretised displacement field, Equation (67), into Equation (30), the virtual work performed by external forces is then given by

$$W_{ext} = \int_{\Gamma_0} \delta \mathbf{u}^T \mathbf{t} dA = \delta \mathbf{u}_e^T \int_{\Gamma_0} \mathbf{N}^T \mathbf{t} dA = \delta \mathbf{u}_e^T \mathbf{g} \quad (71)$$

where the generalised forcing vector \mathbf{g} is given by

$$\mathbf{g} = \int_{\Gamma_0} \mathbf{N}^T \mathbf{t} dA \quad (72)$$

3.5 Gaussian quadrature

For a triangular elements with three nodes, the shape functions, the integrands on equations (64), (66) and (70) are constant inside the element domain. For more complex elements, the integrals are performed using the Gaussian quadrature rule

$$\int_{-1}^{+1} f(x) dx \approx \sum_{i=1}^n w_i f(x_i) \quad (73)$$

where x_i and w_i are the roots and weights of Legendre polynomials respectively. It can be demonstrated the approximation is exact when $f(x)$ is a polynomial function of degree $2n-1$ or lower. The quadrature can be expanded for nested integrals of multivariable functions.

$$\int_{-1}^{+1} \int_{-1}^{+1} f(x, y) dx dy \approx \sum_{i=1}^n \sum_{j=1}^n w_i w_j f(x_i, x_j) \quad (74)$$

4 Numerical example

The equations described above were inserted and developed symbolically in the script *sympy_quad9.py* with aid of the symbolic python library sympy. The script generates automatically the numerical function script *numpy_quad9.py* which calculates the integrands on equations (64), (66) and (70) for a given set of natural coordinates. The equations are integrated numerically within the class script *obj_quad9.py*. A numerical example was performed to test the numerical routines. Figure 6 depicts a 2 m long bar, 50 mm high and clamped at the left extremity. The material is modelled with a Young modulus $E = 70$ GPa, Poisson's ratio $\nu = 0.3$ and density $\rho = 2700$ kg/m³. The loading is applied on the right as a traction in the vertical direction $\mathbf{t} = 3 \cdot 10^6 [\sin(20 \cdot 2\pi t) + \sin(48 \cdot 2\pi t)]$. Figure 7 illustrates the results obtained with the code described and the commercial FEM package COMSOL.

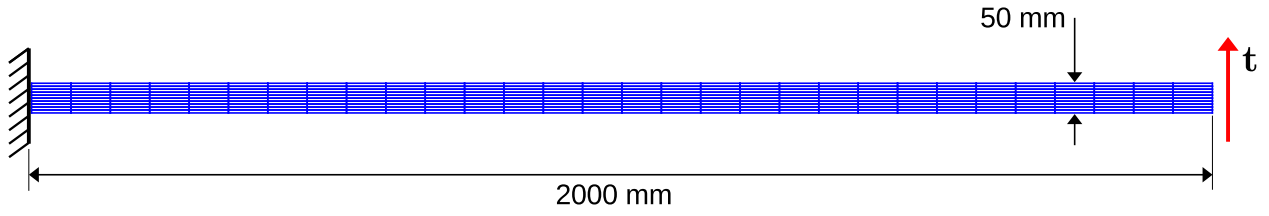


Figure 6: Example

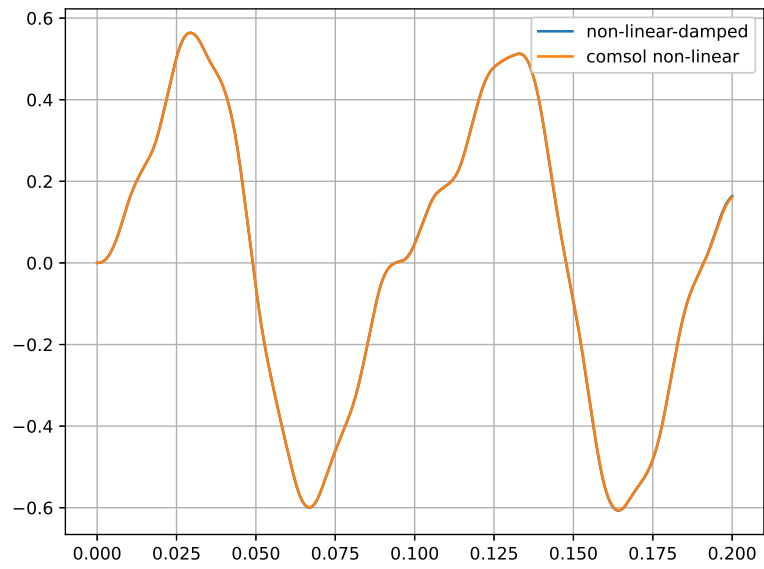


Figure 7: Example results